Desalination and Water Treatment
www.deswater.com

doi: 10.1080/19443994.2013.834519

53 (2015) 84–90
January

Taylor & Francis
Taylor & Francis Group

Manganese ferrite nanoparticle: Synthesis, characterization, and photocatalytic dye degradation ability

Niyaz Mohammad Mahmoodi

Department of Environmental Research, Institute for Color Science and Technology, Tehran, Iran
Tel. +98 021 22969771; Fax: +98 021 22947537; emails: nm_mahmoodi@aut.ac.ir; mahmoodi@icrc.ac.ir

Received 21 April 2013; Accepted 7 August 2013

ABSTRACT

In this paper, manganese ferrite nanoparticle ($MnFe_2O_4$) (MFN) was synthesized. Photocatalytic degradation of dye using MFN and hydrogen peroxide (H_2O_2) from colored wastewater was studied. Reactive dyes, Reactive Red 198 (RR198), and Reactive Red 120 (RR120), were used as model compounds. The characteristics of MFN were investigated using Fourier transform infrared, X-ray diffraction, and scanning electron microscope. Dye degradation was studied using UV-vis spectrophotometer and ion chromatography. The effects of MFN dosage, salt, and initial dye concentration on dye degradation were evaluated. Formate, acetate, and oxalate anions were detected as dominant aliphatic intermediate. Inorganic anions (nitrate and sulfate anions) were detected as the mineralization products of dyes during the degradation processes. The results indicated that the MFN could be used as a magnetic catalyst to degrade reactive dyes from wastewater.

Keywords: Manganese ferrite nanoparticle; Synthesis; Characterization; Dye degradation; Photocatalytic activity

1. Introduction

One of the major concerns of several industries such as textile, paper, plastic, etc. is the presence of dye in their wastewater. They consume water and produce colored wastewater. Some of dyes are difficult to degrade because they have complex structure and synthetic origin. In addition, they may produce toxic or carcinogenic materials by different reactions such as hydrolysis, oxidation, etc. in the environment [1–10].

Advanced oxidation processes (AOPs) degrade pollutants in aqueous media by strong oxidants such as hydroxyl radicals ($HO^{\bullet}$) [11]. An emerging field in AOPs is the application of magnetic catalysts to degrade pollutants. The properties of magnetic catalysts have opened a new field in engineering separations applications. They could be separated based on their nanostructures since the ease of direction of magnetization would vary depending on the ordering of atoms in the magnetic structure [12,13]. The application of iron-based nanoparticles, strong ferromagnets, has been extensively studied. The iron nanoparticles are very effective to remove a wide variety of common environmental organic and inorganic contaminants [12]. Suitable nanoparticles for magnetically assisted separation are the superparamagnetic nanoparticles. The application of a magnetic field of low intensity induces the magnetization of the material and thus makes the use of a magnetic force possible, but when the magnetic field is cut of, the magnetization immediately decreases to zero. This last point is important for the release of particles after adsorption of the waste [14,15].

A literature review showed that the photocatalytic degradation of dyes using manganese ferrite nanoparticle ($MnFe_2O_4$) (MFN) was not investigated in details. In this paper, MFN was synthesized and characterized. The photocatalytic dye degradation ability of MFN from wastewater in presence of hydrogen peroxide (H_2O_2) was studied. Reactive Red 198 (RR198) and Reactive Red 120 (RR120) were used as model dyes. The characteristics of MFN were investigated using Fourier transform infrared (FTIR), X-ray diffraction (XRD), and scanning electron microscope (SEM). Photocatalytic dye degradation was studied by UV-vis spectrophotometer and ion chromatography (IC). The effects of MFN dosage, salt (inorganic anion), and initial dye concentration on photocatalytic dye degradation were evaluated.

2. Experimental

2.1. Chemicals

Reactive Red 198 ($C_{27}H_{18}ClN_7O_{16}S_5Na_4$) and Reactive Red 120 ($C_{44}H_{24}Cl_2N_{14}O_{20}S_6Na_6$) were used as model dyes. The dyes were obtained from Ciba Ltd and used without further purification. The chemical structure of dyes was shown in Fig. 1. Other chemicals were purchased from Merck and used as received.

2.2. Synthesize of MFN

MFN (⩽80 nm) was synthesized in our laboratory. Manganese nitrate (4.90 g) and iron nitrate (13.4 g) was dissolved in 50 mL distilled water and added to aqueous mixed solution (4.2 g NaOH in 70 mL distilled water and 3 mL ethylene diamine (EG)). This solution was heated at 90˚C for 1 h to achieve complete chelation. The powder was calcined on alumina crucible at 500˚C for 1 h, with a heating rate of 10˚C/min.

2.3. Characterization

The functional group of the material was studied using FTIR spectroscopy (Perkin–Elmer Spectrophotometer Spectrum One) in the range 4,000–450 cm^{-1}. Crystallization behavior was identified by XRD model Siemens D-5000 diffractometer with Cu K_α radiation ($\lambda = 1.5406 Å$) at room temperature. The morphological structure of the material was examined by SEM using a LEO 1455VP scanning microscope.

2.4. Photocatalytic reactor

Experiments were carried out in a batch mode photoreactor. The irradiation source was a UV–C lamp (200–280 nm, 9 W, Philips), which was placed in the inner quartz tube of the reactor.

2.5. Photocatalytic dye degradation

The photocatalytic dye degradation experiments were conducted by mixing various amounts of MFN (0–0.2 g) in photoreactor containing 800 mL of a dye solution (100 mg/L) and H_2O_2 (1.2 mM) and 25˚C. The solution samples were withdrawn from the reaction medium at regular time intervals. The MFN was separated from solution using magnetic force and the change on the absorbance at maximum wavelength

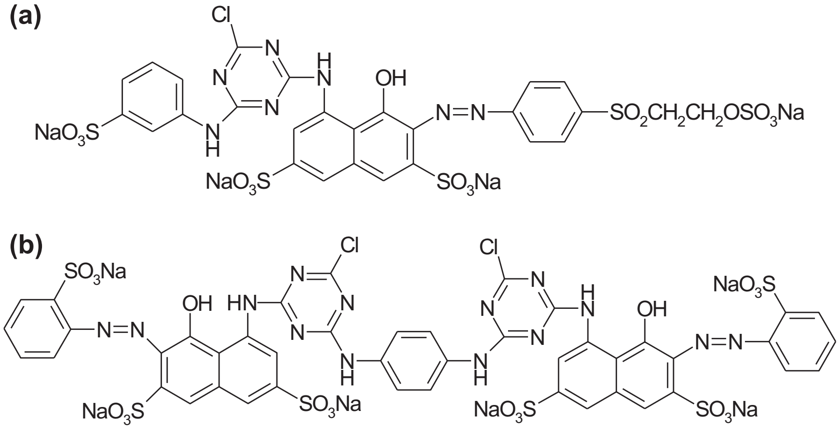

Fig. 1. The chemical structure of dyes (a) RR198 and (b) RR120.

(λ_{max}) of dyes (520 nm for RR198 and 514 nm for RR120) was monitored by UV-vis spectrophotometer (Perkin–Elmer Lambda 25).

The effect of MFN dosages on the photocatalytic dye degradation was investigated by contacting 800 mL of dye solution (100 mg/L) and H_2O_2 (1.2 mM) at room temperature (25˚C) for 60 min. Different amounts of MFN (0, 0.05, 0.10, 0.15, and 0.20 g) were applied.

The effect of initial dye concentration on the photocatalytic dye degradation was studied. The MFN was added to 800 mL of different dye concentrations (100, 150, 200, and 250 mg/L) and H_2O_2 (1.2 mM).

The effect of salt on the photocatalytic dye degradation was studied. About 0.02 M of different salts (Na_2SO_4, NaCl, $NaHCO_3$, and Na_2CO_3) was added to 800 mL of dye solution (100 mg/L) containing H_2O_2 (1.2 mM) and MFN at room temperature (25˚C).

Ion chromatograph (METROHM 761 Compact IC) was used to assay the appearance of carboxylic acids, nitrate, and sulfate ions formed during the degradation and mineralization of dyes (Solution: 800 mL, Dye: 100 mg/L, MFN at room temperature (25˚C)) using a METROSEP anion dual 2, flow 0.8 ml/min, 2 mM $NaHCO_3$/1.3 mM Na_2CO_3 as eluent, temperature 20˚C, pressure 3.4 MPa, and conductivity detector.

3. Results and discussion

3.1. Characterization

The FTIR spectrum of MFN in the wavelength ranges from 4,000 to 400cm^{-1} is shown in Fig. 2. In FTIR spectrum of MFN, a broad absorption band around 3400 cm^{-1} and less intensive band at 1620 cm^{-1} are attributed to the stretching vibration of the hydrogen-bonded O–H groups [16,17]. The peak at 600–500 cm^{-1} is due to the metal–oxygen bond [17].

Fig. 3 illustrates the XRD pattern of the MFN. The results showed that spinel was formed as the most intense (311) peak and Miller indices (220), (222), (400), (422), (511), and (440) matched well with the reflections of the manganese ferrite reported in the previous published paper [17].

SEM has been a primary tool for characterizing the surface morphology and fundamental physical properties of material surface. It is useful for determining the particle shape, and appropriate size distribution of the material. The SEM micrograph of the MFN (Fig. 4) shows a relatively homogeneous particle size distribution of MFN.

3.2. Effects of operational parameters on dye degradation

3.2.1. Effect of MFN dosage

Fig. 5 shows the effect of MFN dosage on the photocatalytic dye degradation. The photocatalytic degradation with H_2O_2 in the absence of MFN is 53 and 50% for RR198 and RR120, respectively (Fig. 5). Considering that the hydrogen peroxide alone is not effective to oxidize dyes in the colored wastewater samples, it needs to be activated by MFN, which played predominant roles in its integrated treatment. It is observed that the simultaneous use of MFN and H_2O_2 to a certain extent yielded a significant

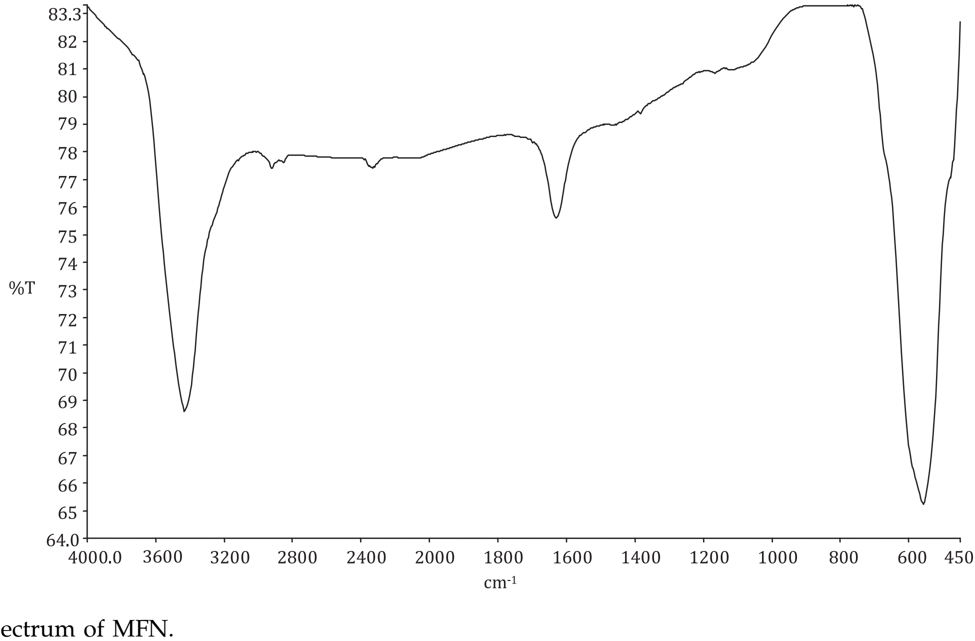

Fig. 2. FTIR spectrum of MFN.

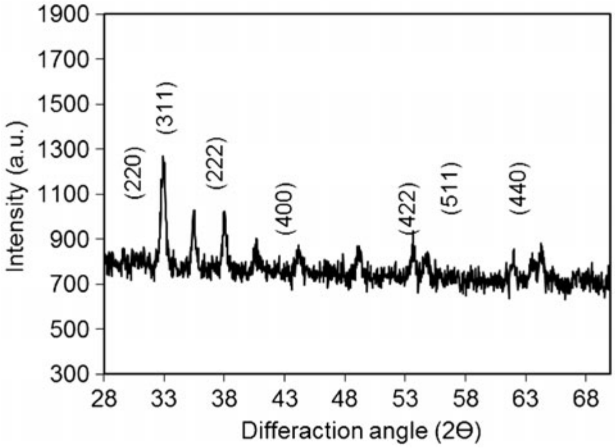

Fig. 3. XRD pattern of MFN.

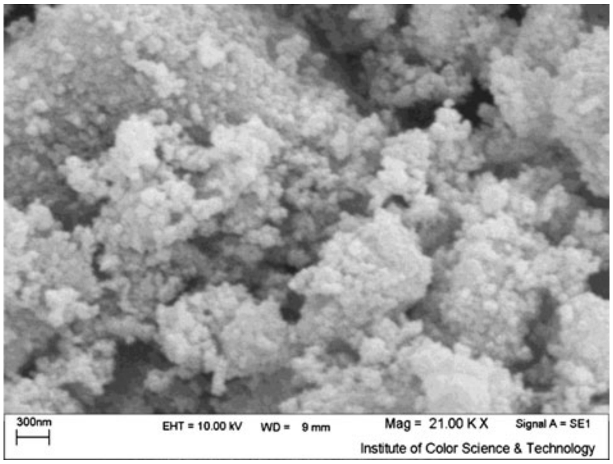

Fig. 4. SEM image of MFN.

improvement of dye degradation compared to that of the H_2O_2 degradation alone (Fig. 5).

The photocatalytic degradation mechanism of organics using MFN is as follows: hydrogen peroxide can be activated on the MFN surface to generate hydroxyl radicals. The MFN can be regarded to function as an electron-transfer catalyst involving the reduced and oxidized catalyst states (Reactions (1) and (2)).

$$MnFe_2O_4 + H_2O_2 \rightarrow MnFe_2O_4^+ + HO^- + HO^{\bullet} \tag{1}$$

$$MnFe_2O_4^+ + H_2O_2 \rightarrow MnFe_2O_4 + HO_2^{\bullet} + H^+ \tag{2}$$

3.2.4. Effect of salt

The occurrence of salt (inorganic anion) is rather common in dye-containing industrial wastewater. These substances may compete for the active sites on the MFN surface or deactivate the MFN and, subsequently, decrease the degradation rate of the target dyes. A major drawback resulting from the high reactivity and nonselectivity of $HO^{\bullet}$ is that it also reacts with nontarget compounds present in the background water matrix, i.e. dye auxiliaries present in the dye bath. It results higher $HO^{\bullet}$ demand to accomplish the desired degree of degradation, or complete inhibition of advanced degradation rate and efficiency [18].

Fig. 6 shows the effect of salts on the photocatalytic dye degradation using MFN. Of the anionic species studied (Na_2SO_4, NaCl, $NaHCO_3$, and Na_2CO_3), carbonate and bicarbonate exhibited the inhibition effect. Although their presence could inhibit H_2O_2 degradation through their scavenging effects on the $HO^{\bullet}$ radicals, the bicarbonates ions could prevent the reduction of pH following catalytic degradation. To generate

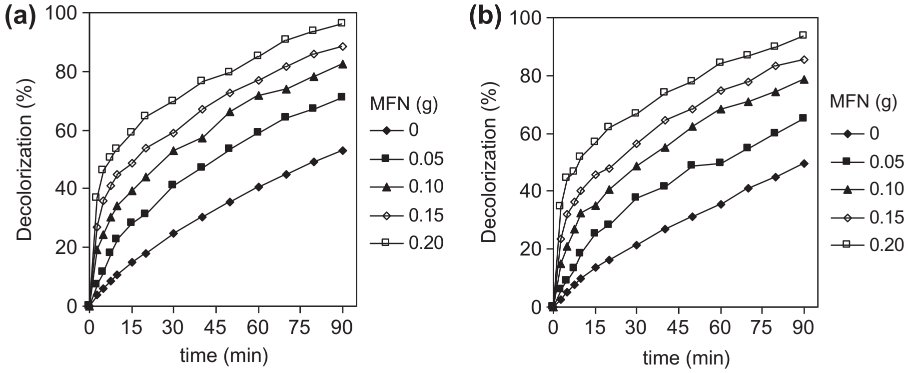

Fig. 5. The effect of MFN dosage on the photocatalytic degradation of dyes using UV/MFN/H_2O_2 (a) RR198 and (b) RR120.

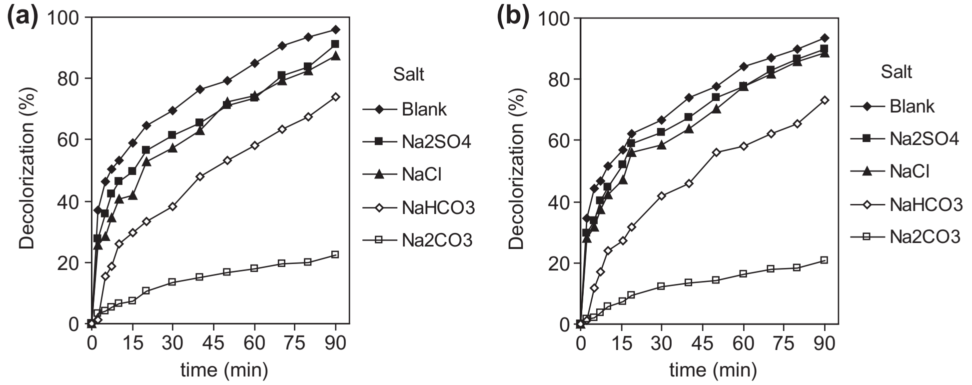

Fig. 6. The effect of salt (inorganic anion) on the photocatalytic degradation of dyes using UV/MFN/H_2O_2 (a) RR198 and (b) RR120.

sufficient levels of HO$^•$ for the photocatalytic dye degradation in the presence of high levels of bicarbonate and carbonate, a higher oxidant dose should be used [18,19].

3.2.2. Effect of initial dye concentration

To study the effect of dye concentration on the rate of the photocatalytic dye degradation, the dye concentration was varied from 100 to 250 mg/L while the other variables were kept constant. Fig. 7 shows the photocatalytic dye degradation for the various initial dye concentrations at different time intervals. With the increase in the dye concentration, the possible cause is the interference from intermediates formed upon degradation of the parental dye molecules. Such suppression would be more pronounced in the presence of an elevated level of degradation intermediates formed upon an increased initial dye concentration [19].

3.3. Degradation and mineralization of dyes

Degradation of dye should be evaluated as an overall destruction process, involving the degradation of both the parent dye and its intermediates. Hydroxylation of aromatic intermediates produced during the degradation process leads to the cleavage of the aromatic ring and the formation of oxygen-containing aliphatic compounds [20]. During the degradation of RR198 and RR120 using UV/MFN/H_2O_2 and UV/H_2O_2, various intermediates (Formate, acetate, and oxalate) were detected as important aliphatic carboxylic acid intermediates (Fig. 8). The results show that UV/MFN/H_2O_2 has higher dye degradation efficiency than that of UV/H_2O_2 due to the catalytic effect of MFN. The formation of carboxylic acids initially increased with the illumination time, and then dropped. Carboxylic acids can react directly with oxidants and generate CO_2.

Also, the mineralization of dye using photocatalytic degradation using UV/MFN/H_2O_2 implies the appearance of inorganic products, mainly anions,

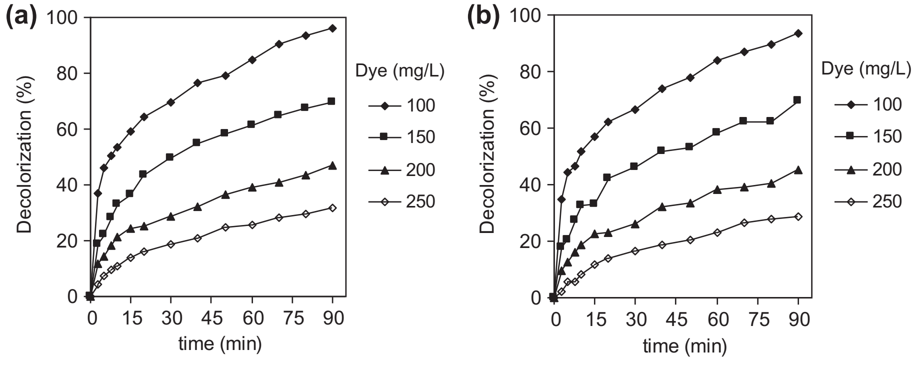

Fig. 7. The effect of dye concentration on the photocatalytic degradation of dyes using UV/MFN/H_2O_2 (a) RR198 and (b) RR120.

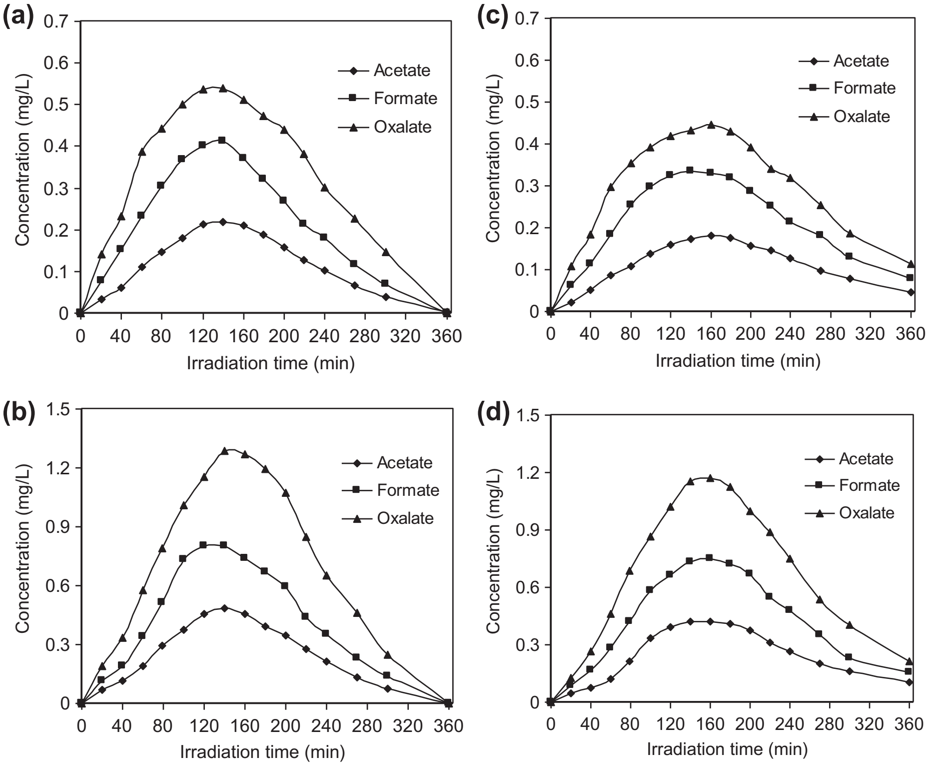

Fig. 8. Formation and disappearance of aliphatic carboxylic acids during the degradation of dyes using UV/MFN/H_2O_2 ((a) RR198 and (b) RR120) and UV/H_2O_2 ((c) RR198 and (d) RR120).

since hetero-atoms are generally converted into anions in which they are at their highest degradation degree. The dye degradation leads to the conversion of organic carbon into harmless gaseous CO_2 and that of N and S into inorganic ions, such as nitrate and sulfate ions, respectively [19,21]. Mineralization of dyes was checked for an irradiation period of 200 min. The formation of NO_3^- and SO_4^{2-} from dye mineralization of RR120 and RR198 was shown in Fig. 9.

The quantity of released nitrate ions (RR198: 0.5800 mM and RR120: 0.7630 mM) during the mineralization of dyes by UV/MFN/H_2O_2 is lower than that expected from stoichiometry (RR198: 0.7119 mM and RR120: 0.9534 mM) indicating that N-containing species remain adsorbed in the MFN surface or most probably, that significant quantities of N_2 and/or NH_3 have been produced and transferred to the gas phase. Nitrogen atom is in its + 1 degradation degree in the

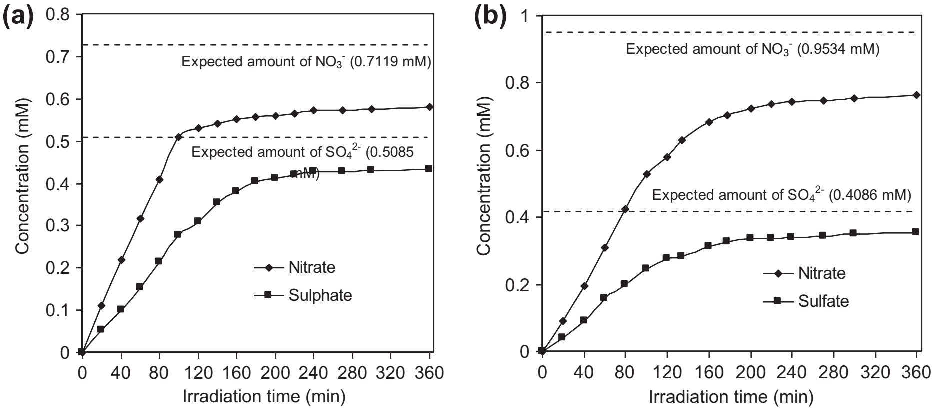

Fig. 9. Evolution of inorganic ions during the mineralization of dyes using UV/MFN/H_2O_2 (a) RR198 and (b) RR120).

azo bonds. This degradation degree favors the evolution of gaseous N_2 by the two-step reduction process expressed previously. N_2 evolution is the ideal case for a decontamination reaction involving totally innocuous nitrogen-containing final product.

Finally, the quantity of released sulfate ions (RR198: 0.4340 mM and RR120: 0.3530 mM) during the mineralization of dyes by UV/MFN/H_2O_2 is lower than that expected from stoichiometry (RR198: 0.5085 mM and RR120: 0.4086 mM). This could be first explained by a loss of sulfur-containing volatile compounds such as H_2S and/or SO_2. However, this is not probable since both gases are very soluble in water and known as readily oxidizable into sulfate by photocatalytic ozonation. The more probable explanation for the quantity of SO_4^{2-} obtained smaller than that expected from stoichiometry is given by the partially irreversible adsorption of some SO_4^{2-} ions at the surface of MFN as already observed [18].

4. Conclusions

In this paper, MFN was synthesized and characterized. The photocatalytic dye degradation ability of MFN in the presence of hydrogen peroxide (H_2O_2) from colored textile wastewater was studied. Reactive dyes were used as model compounds. The effects of MFN dosage, initial dye concentration, and salt on photocatalytic dye degradation were evaluated. The photodegradation with H_2O_2 in the absence of MFN presents a low performance for dye degradation from solutions. The synergistic effects of MFN and H_2O_2 were observed because of the catalytically performance of MFN for decomposition of hydrogen peroxide into hydroxyl radicals. Formate, acetate, and oxalate anions were detected as dominant aliphatic intermediate. Nitrate and sulfate anions were detected as the mineralization products of dyes during the degradation processes. It can be concluded that the MFN could be used as magnetic catalyst to degrade dyes from wastewater.

References

[1] B.S. Ooi, J.Y. Sum, S.O. Lai, Investigation on membrane morphological and chemical properties changes at different reaction times and its effect on dye removal, Desalin. Water Treat. 45 (2012) 250–255.

[2] B. Hayati, N.M. Mahmoodi, Modification of activated carbon by alkaline to remove dyes from wastewater: Mechanism, isotherm and kinetic, Desalin. Water Treat. 47 (2012) 322–333.

[3] L.W. Man, P. Kumar, T.T. Teng, K.L. Wasewar, Design of experiments for Malachite Green dye removal from wastewater using thermolysis—Coagulation—flocculation, Desalin. Water Treat. 40 (2012) 260–271.

[4] S. Sivrikaya, S. Albayrak, M. Imamoglu, A. Gundogdu, C. Duran, H. Yildiz, Dehydrated hazelnut husk carbon: A novel sorbent for removal of Ni(II) ions from aqueous solution, Desalin. Water Treat. 50 (2012) 2–13.

[5] N.M. Mahmoodi, Magnetic ferrite nanoparticle—alginate composite: Synthesis, characterization and binary system dye removal, J. Taiwan Inst. Chem. Eng. 44 (2013) 321–329.

[6] N.M. Mahmoodi, Equilibrium, kinetic and thermodynamic of dye removal using alginate from binary system, J. Chem. Eng. Data. 56 (2011) 2802–2811.

[7] N.M. Mahmoodi, Photocatalytic ozonation of dyes using copper ferrite nanoparticle prepared by co-precipitation method, Desalination 279 (2011) 332–337.

[8] N. Atar, A. Olgun, F. Çolak, Thermodynamic, equilibrium and kinetic study of the biosorption of basic blue 41 using Bacillus maceran, Eng. Life Sci. 8 (2008) 499–506.

[9] Y. Bulut, H. Aydin, A kinetics and thermodynamics study of methylene blue adsorption on wheat shells, Desalination 194 (2006) 259–267.

[10] H. Parab, M. Sudersanan, N. Shenoy, T. Pathare, B. Vaze, Use of agro-industrial wastes for removal of basic dyes from aqueous solutions, Clean - Soil, Air Water. 37 (2009) 963–969.

[11] T.A. Kurniawan, W.H. Lo, Removal of refractory compounds from stabilized landfill leachate using an integrated H_2O_2 oxidation and granular activated carbon (GAC) adsorption treatment, Water Res. 43 (2009) 4079–4091.

[12] R.D. Ambashta, M. Sillanpää, Water purification using magnetic assistance: A review, J. Hazard. Mater. 180 (2010) 38–49.

[13] J. Sun, R. Xu, Y. Zhang, M. Ma, N. Gu, Magnetic nanoparticles separation based on nanostructures, J. Magn. Magn. Mater. 312 (2007) 354–358.

[14] A.F. Ngomsik, A. Bee, M. Draye, G. Cote, V. Cabuil, Magnetic nano and microparticles for metal removal and environmental applications: A review, C. R. Chimie. 8 (2005) 963–970.

[15] S. Thurm, S. Odenbach, Magnetic separation of ferrofluids, J. Magn. Magn. Mater. 252 (2002) 247–249.

[16] D.L. Pavia, G.M. Lampman, G.S. Kaiz, Introduction to Spectroscopy: A Guide for Students of Organic Chemistry, W.B. Saunders Company, Philadelphia, 1987.

[17] P. Laokul, V. Amornnkitbamrung, S. Serphin, S. Maensiri, Characterization and magnetic properties of nanocrystalline $CuFe_2O_4$, $NiFe_2O_4$ and $ZnFe_2O_4$ powders prepared by the Aloe vera extract solution, Current Appl. Physics. 11 (2011) 101–108.

[18] I. Arsalan-Alaton, A review of the effects of dye-assisting chemicals on advanced oxidation of reactive dyes in wastewater, Color. Technol. 119 (2003) 345–353.

[19] I.K. Konstantinou, T.A. Albanis, TiO_2-assisted photocatalytic degradation of azo dyes in aqueous solution: Kinetic and mechanistic investigations—a review, Appl. Catal. B: Environ. 49 (2004) 1–14.

[20] K. Tanaka, S.M. Robledo, T. Hisanaga, R. Ali, Z. Ramli, W.A. Bakar, Photocatalytic degradation of 3,4-xylyl N-methylcarbamate (MPMC) and other carbamate pesticides in aqueous TiO_2 suspensions, J. Mol. Catal. A: Chem. 144 (1999) 425–430.

[21] A. Houas, H. Lachheb, M. Ksibi, E. Elaloui, C. Guillard, J.M. Hermann, Photocatalytic degradation pathway of methylene blue in water, Appl. Catal. B: Environ. 31 (2001) 145–157.